Environmental noise monitoring at AdV+

Soumen Koley, Jan Harms, Irene Fiori, Maria Tringali, Tomek Bulik, Mariusz Suchenek et al.

EGO European Gravitational Observatory

GSI GRAN SASSO SCIENCE INSTITUTE

CENTER FOR ADVANCED STUDIES INFN

Contents

3/14/2023

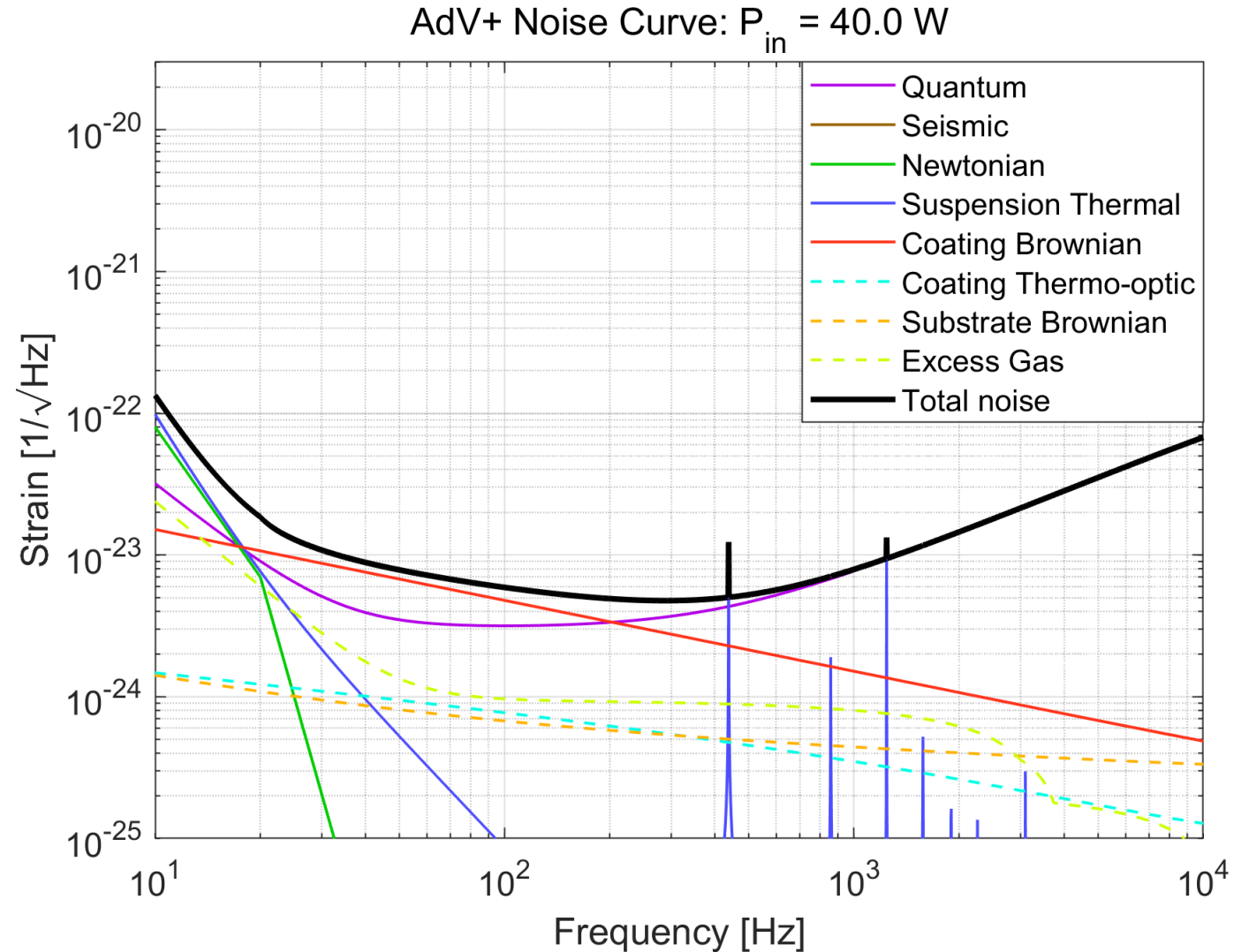# AdV Noise budget

- Radiation pressure noise and shot noise were the fundamental limits to the detector sensitivity during O3
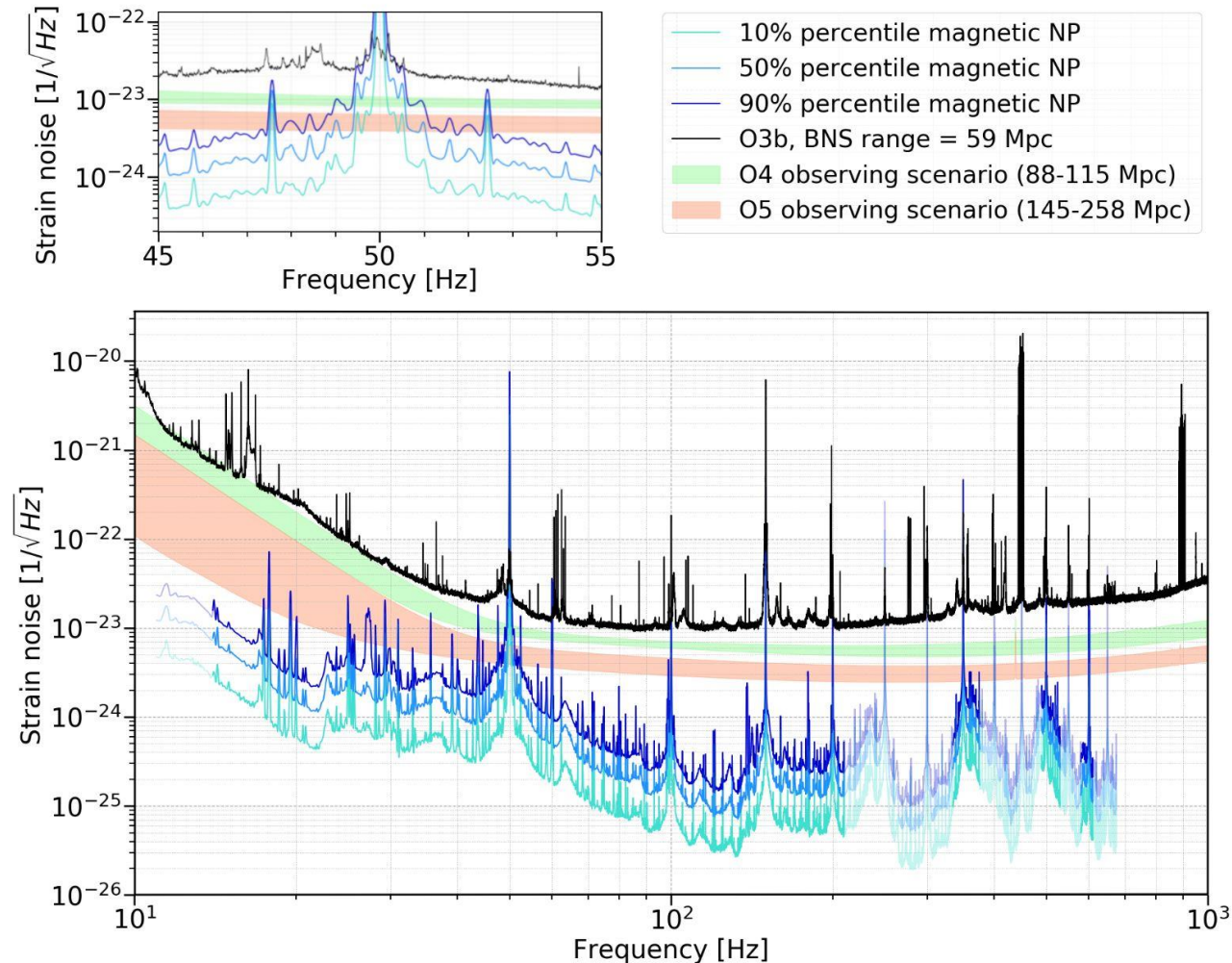

AdV Noise Curve: P_{in} = 18.0 W
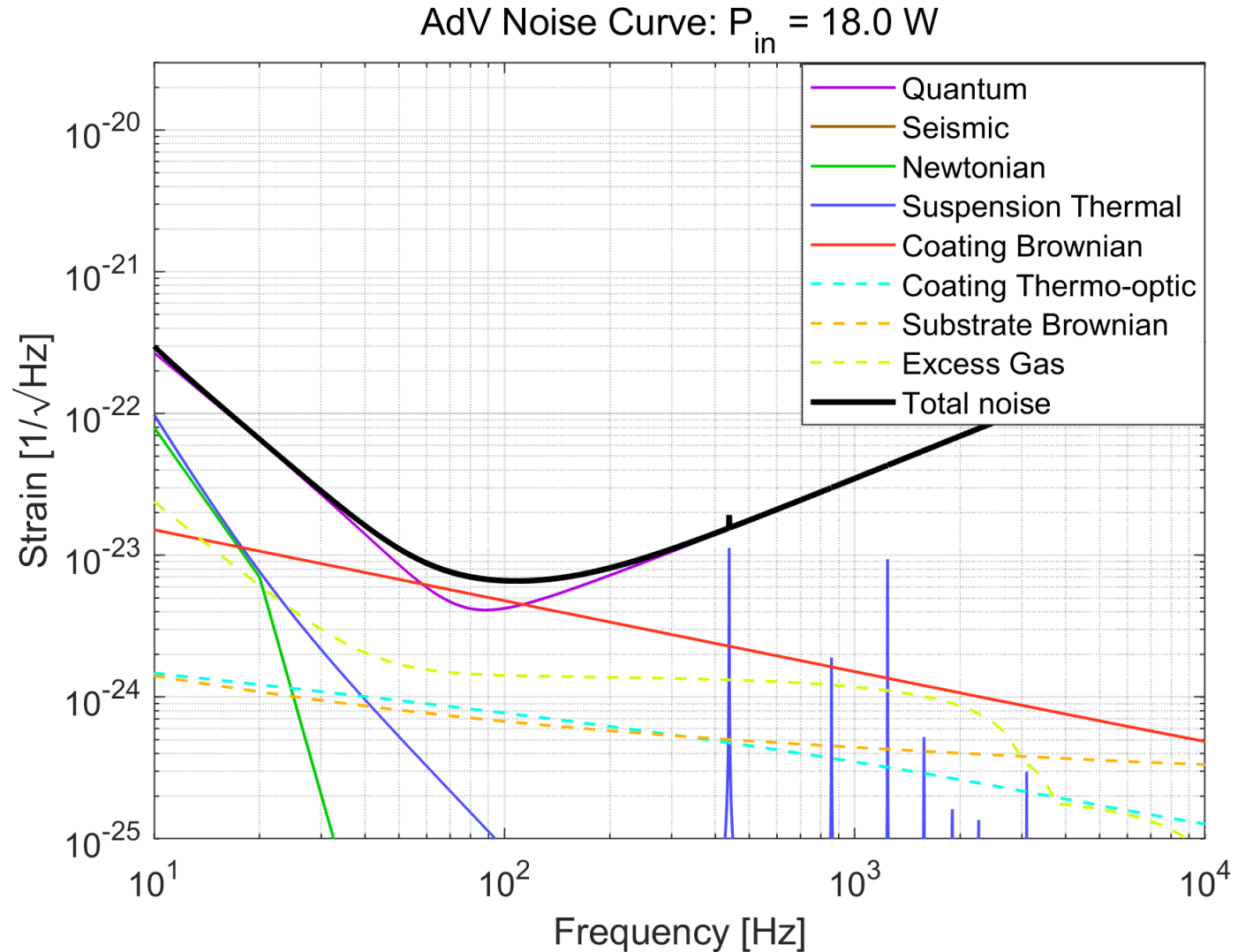
AdV+ Noise budget

- Newtonian noise is expected to have dominant contribution to the O4b sensitivity (lower limit)

AdV+ Noise Curve: P_{in} = 40.0 W

AdV+ Magnetic noise projection

- Magnetic noise is expected to limit several frequency bands during O5 ([Fiori et al, 2020](#))

Newtonian noise - fundamentals

- Mirror acceleration

  - $\delta\vec{a}(\vec{r_0}, t) = G \int dV \, \rho(\vec{r}) \times \frac{1}{|\vec{r}-\vec{r_0}|^3}\left(\xi(\vec{r}, t) - 3\left(\vec{e}_{rr_0}\xi(\vec{r}, t)\right)\right)\vec{e}_{rr_0}$,

    where $\xi(\vec{r}, t)$ is the seismic displacement field, ρ the density and $\vec{e}_{rr_0} = (\vec{r} - \vec{r_0})/|\vec{r} - \vec{r_0}|$

  - Relies on finite element/difference simulations of elastic wave equation

  - Elastic properties of the medium and the noise source properties need to be known

- For surface detectors, the linear dependence of NN and seismic surface displacement allows for designing a Wiener filter given by the residual

  - $R(\omega) = 1 - \frac{\overrightarrow{C_{SN}}(\omega).\left(\overrightarrow{C_{SS}}(\omega)\right)^{-1}.\overrightarrow{C_{NS}}(\omega)}{C_{NN}(\omega)}$, where $\vec{C}_{SN}, \vec{C}_{SS}, \vec{C}_{NN}$,
   correspond to the cross and auto-spectral densities between observed seismic noise and 'expected' Newtonian noise (Badaracco & Harms 2019)
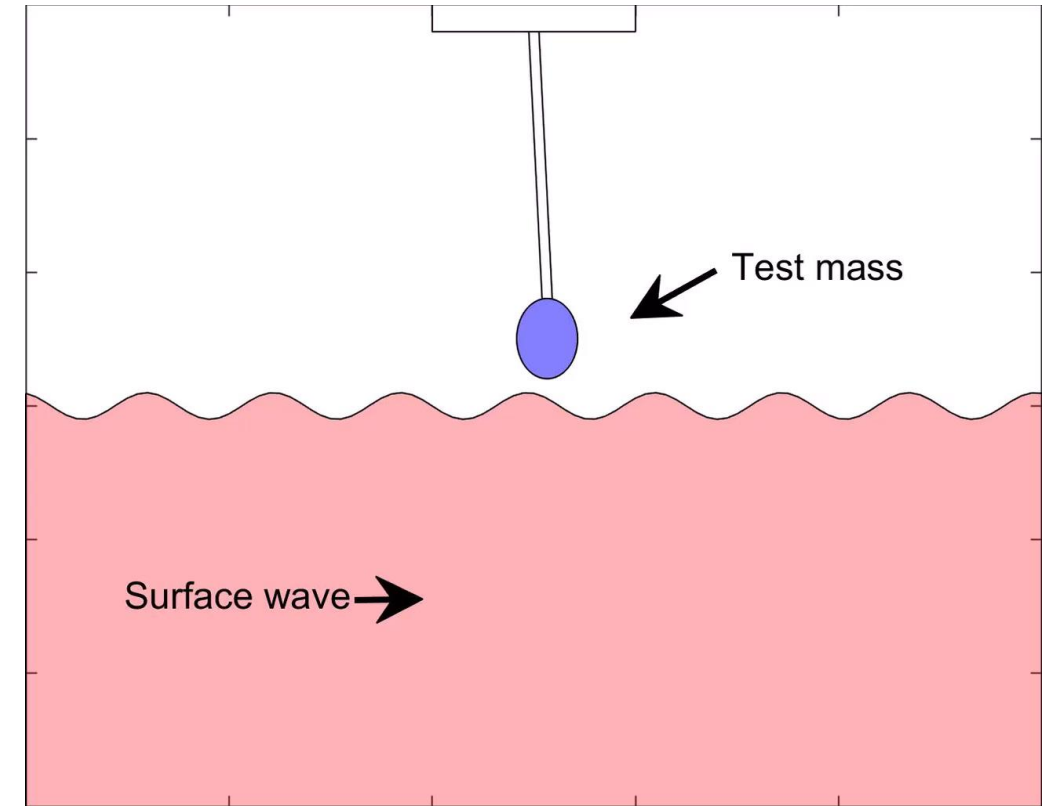
*A toy representation of seismic surface wave inducing mirror motion due to gravitational coupling, $v = 25 m/s \, f = 20 \, Hz$*

Newtonian noise cancellation – Central Building Array layout

- A total of 55, 5 Hz geophones deployed in the central building (CEB)
  - 15 geophones level 1
  - 40 geophones level 2

- Station positions were updated in May 2022 for optimal Newtonian noise cancellation
 - Data acquired continuously at 500 sps and integrated with Virgo DAQ
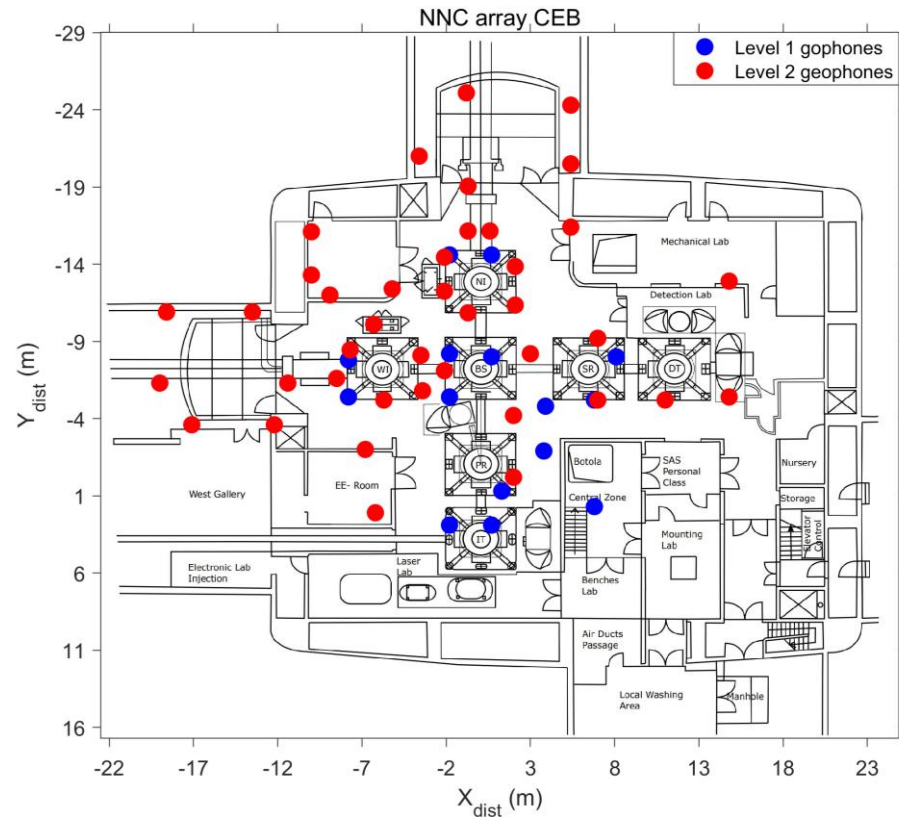
Geophone locations in the CEB prior to the upgrade in May 2022; The blue and the red dots represent the level 1 and level 2 geophones respectively
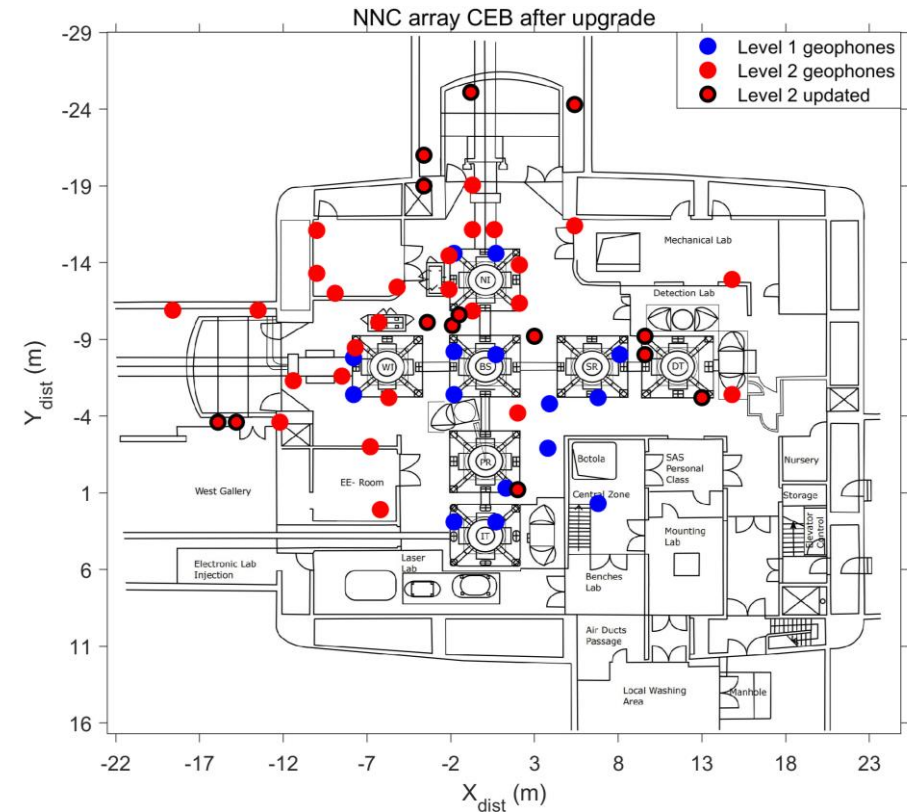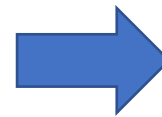
Geophone locations in the CEB after the upgrade in May 2022; Red dots with black edges correspond to the geophones whose positions were changed

Newtonian noise cancellation – End Buildings Array layout

- A total of 30, 5 Hz geophones deployed in the West End Building (WEB)

- A total of 28, 5 Hz geophones deployed in the North End Building (NEB)
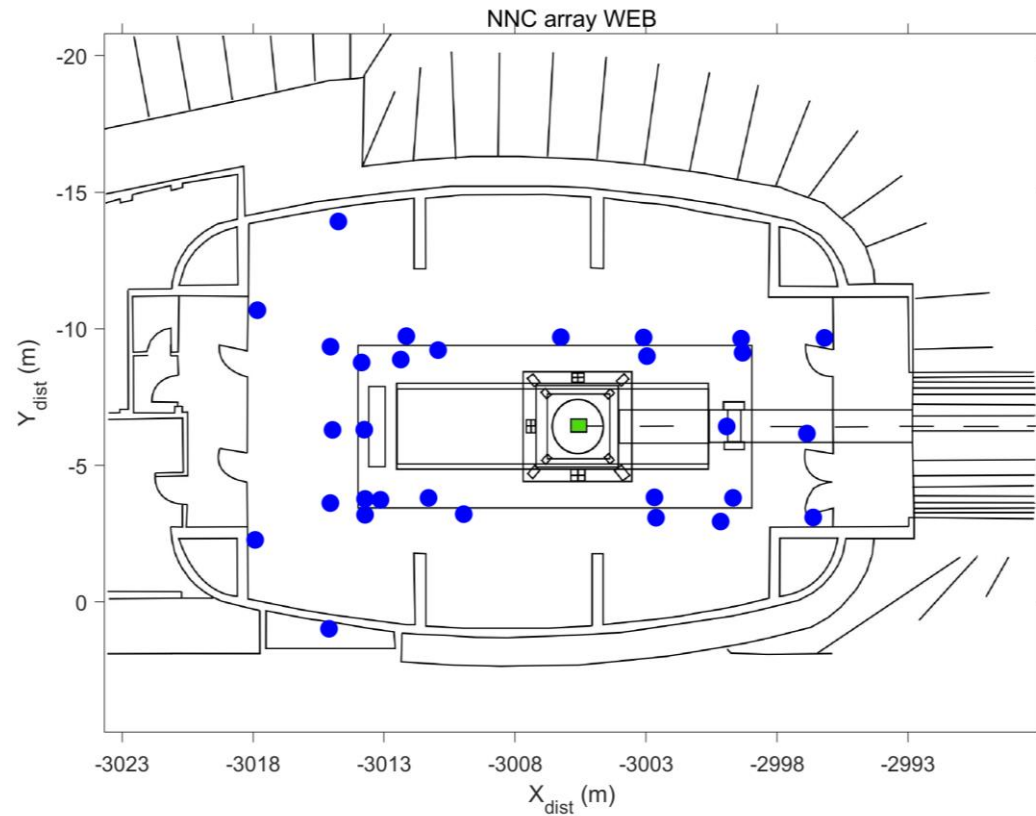
Geophone locations in the WEB represented using the blue dots; Coordinate system origin at the CEB beamsplitter
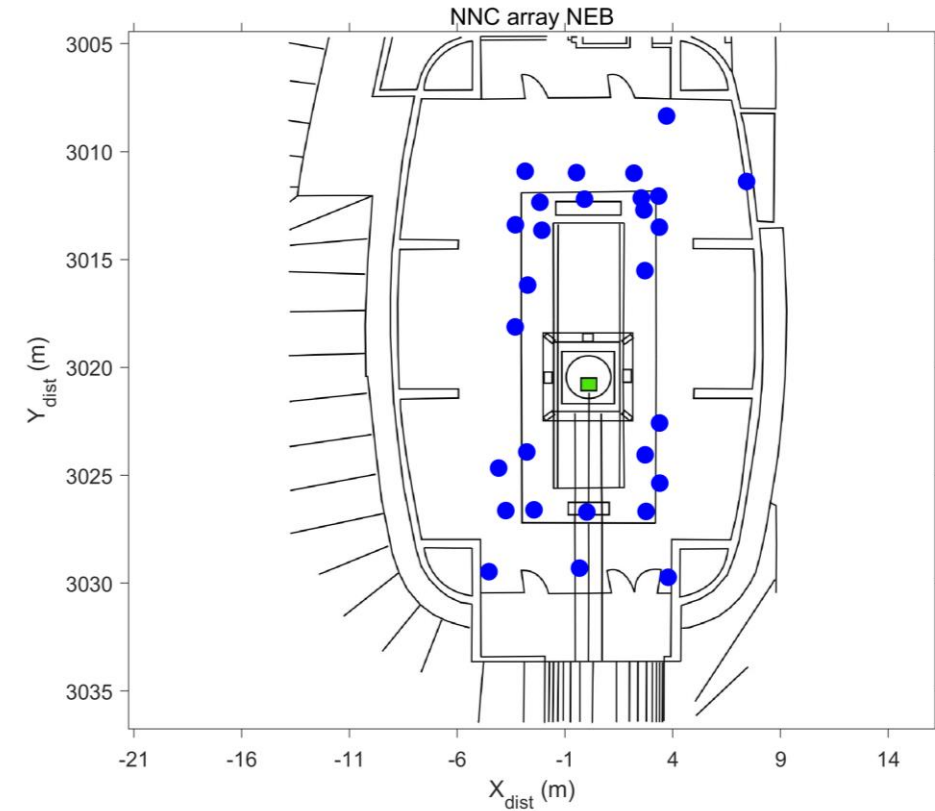
Geophone locations in the NEB represented using the blue dots; Coordinate system origin at the CEB beamsplitter

NNC array – Noise PSD characteristics

- Performance of the NNC 5 Hz geophones are comparable to the GURALP seismometer in the CEB down to 0.4 Hz

- Spatial variation between 10-20 dB for frequencies between 10-20 Hz
- Both broadband and sharp spectral noise observed
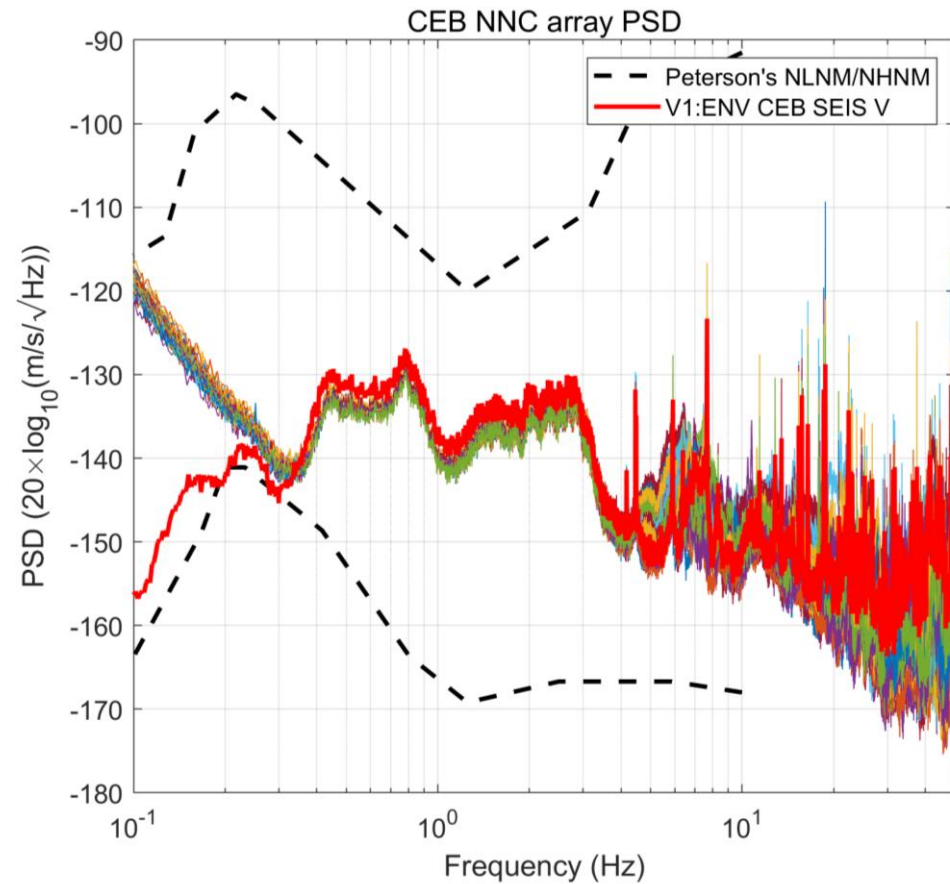
`Mode of the PSD estimates for the CEB NNC geophones and the CEB GURALP seismometer (red curve) starting at GPS time 1359417600; PSD win length 600 s, 300 s overlap, total duration 86400 s
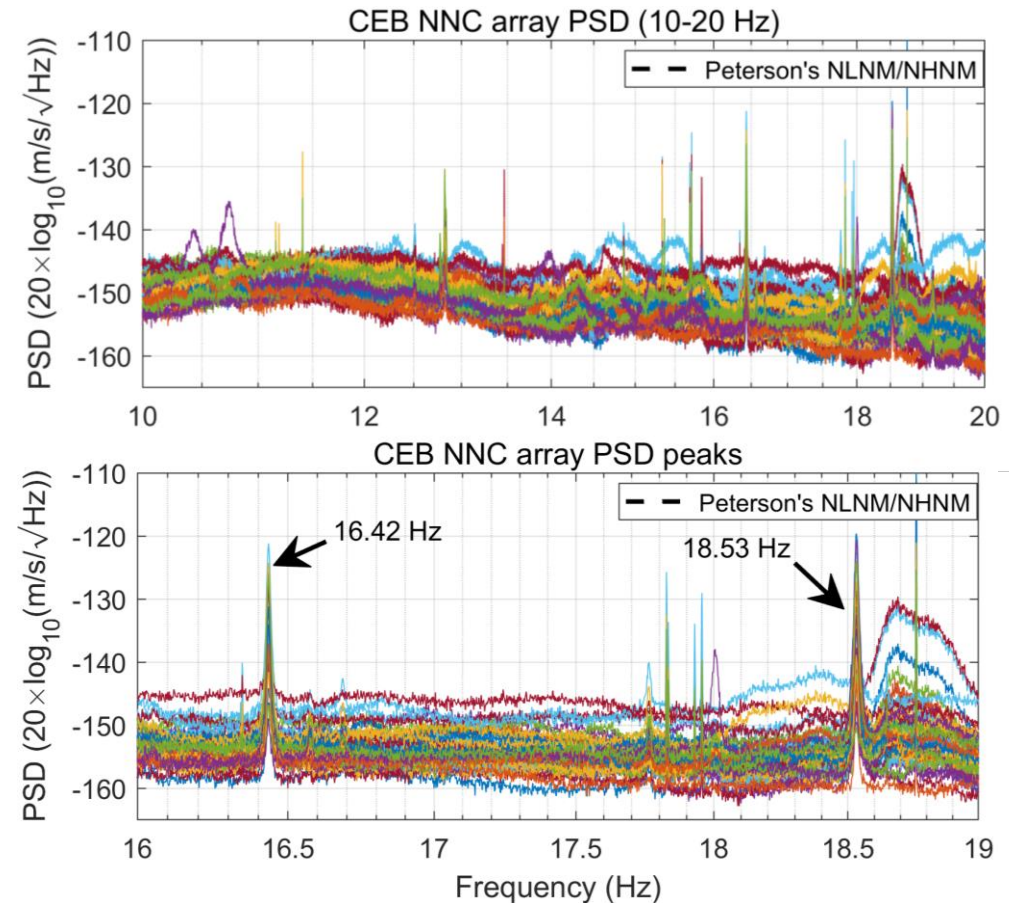
Seismic noise in band 10-40 Hz is composed of broadband as well as sharp spectral noise originating from machines at the site

Noise characteristics – day-night variation

- Maximum seismic noise PSDs are observed at around noon every-day
- An order of magnitude difference in PSDs can be observed between noisy and quiet times, especially in the frequency band 2-6 Hz

- For frequencies above 10 Hz a factor 4-5 difference in PSDs are observed
- Above 20 Hz most noises are generated by machinery at the site and a day-night variation is not observed
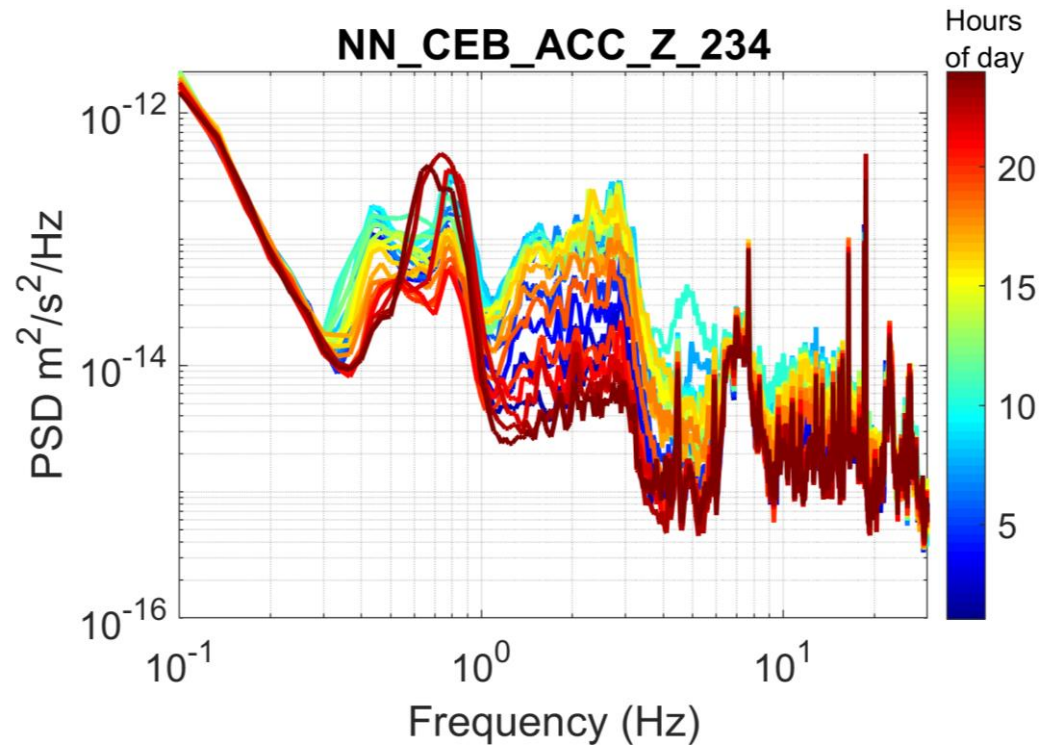
Average PSDs estimated every hour of the day showing strong diurnal variation between 2-15 Hz
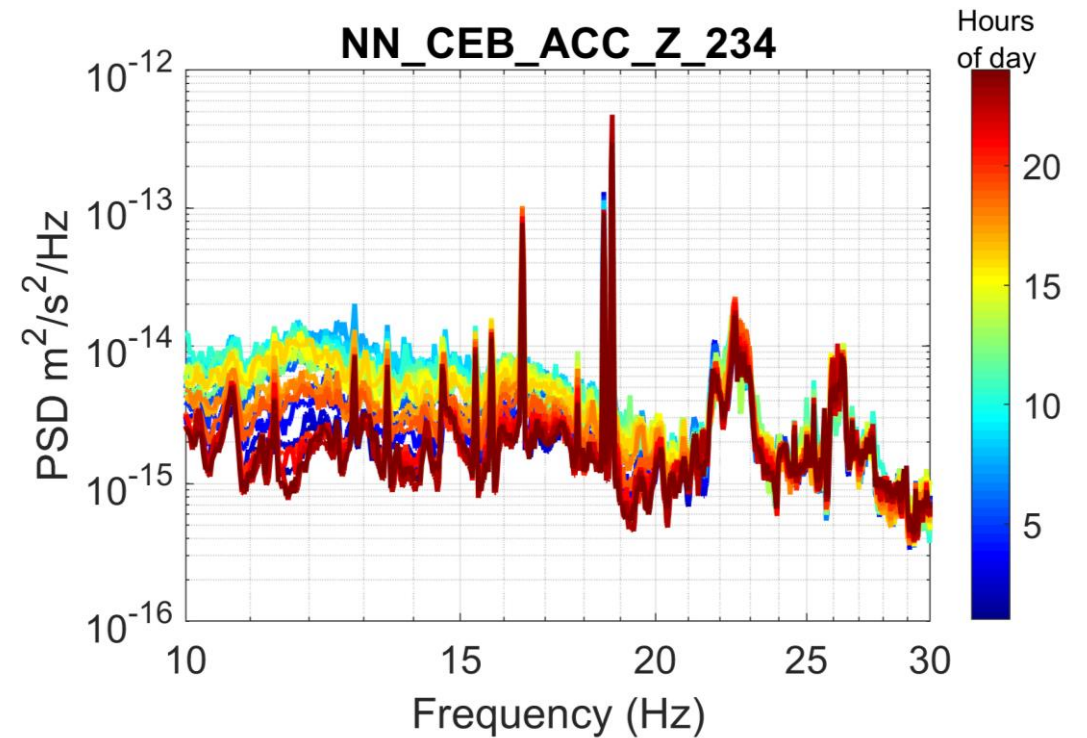
Average PSDs estimated every hour of the day showing weak or no diurnal variation for frequencies greater than 25 Hz

Noise PSD characteristics – Spatial variation in the 2-3 Hz band
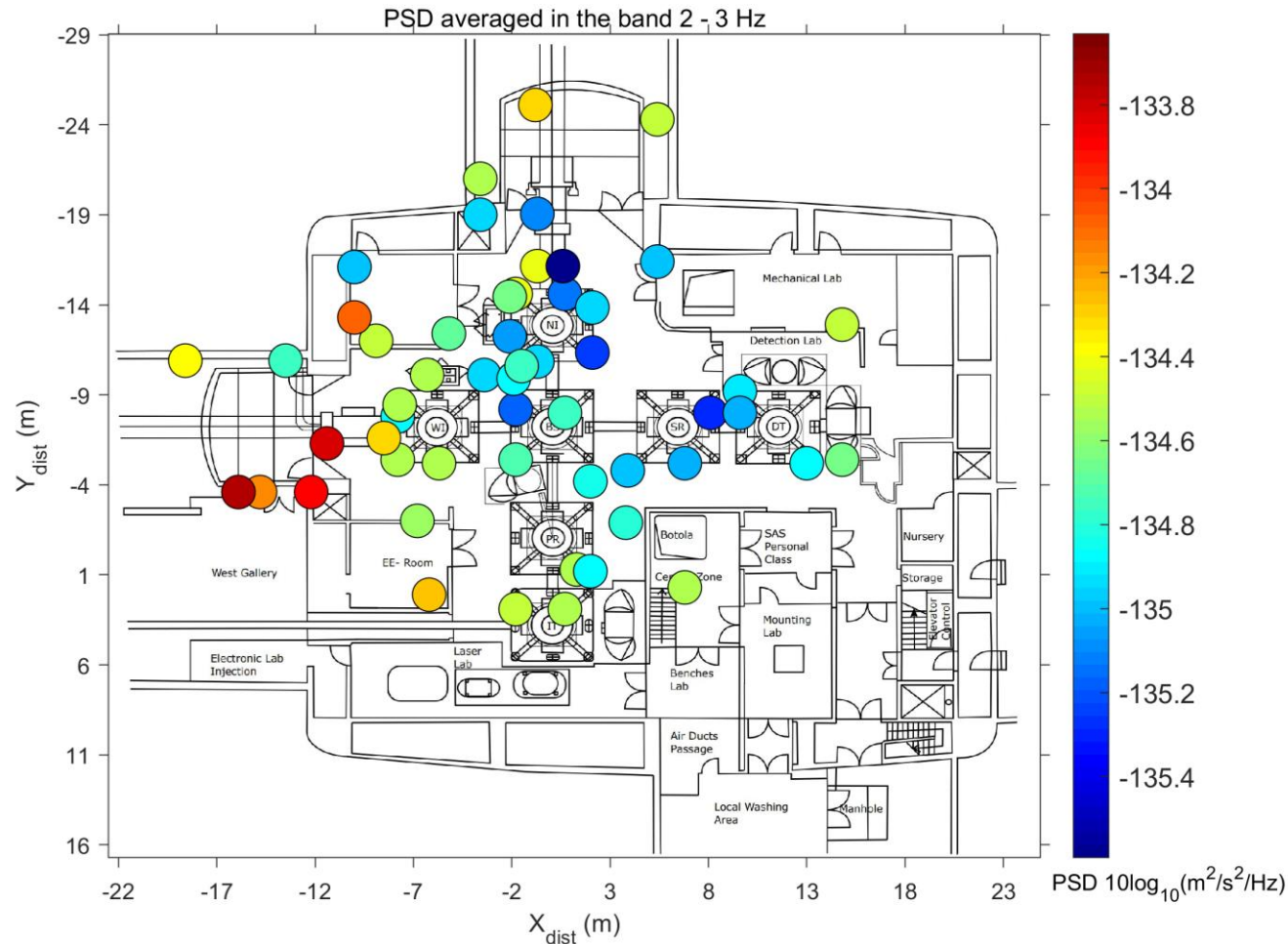
Spatial distribution of seismic noise PSDs averaged in the frequency band 2-3 Hz.

- PSDs computed every 600 s with an overlap of 300 s between consecutive windows

  - Averaged for a week of data

  - Starting time – 1359417618 s

- Spatial variation of the noise PSDs are within 2 dBs

- Noise originates far-away from sources like roads, bridges etc.

  - Little attenuation while propagating through the NNC array

Noise PSD characteristics – Spatial variation in the 10 - 15 Hz band

Spatial distribution of seismic noise PSDs averaged in the frequency band 10-15 Hz.

- Noise PSDs averaged in the frequency band 10-15 Hz show a variation of about 7 dB

  - About 2-3 dB lower than that observed for the 6-8 Hz band

- Noise propagation "dominantly" SE - NW

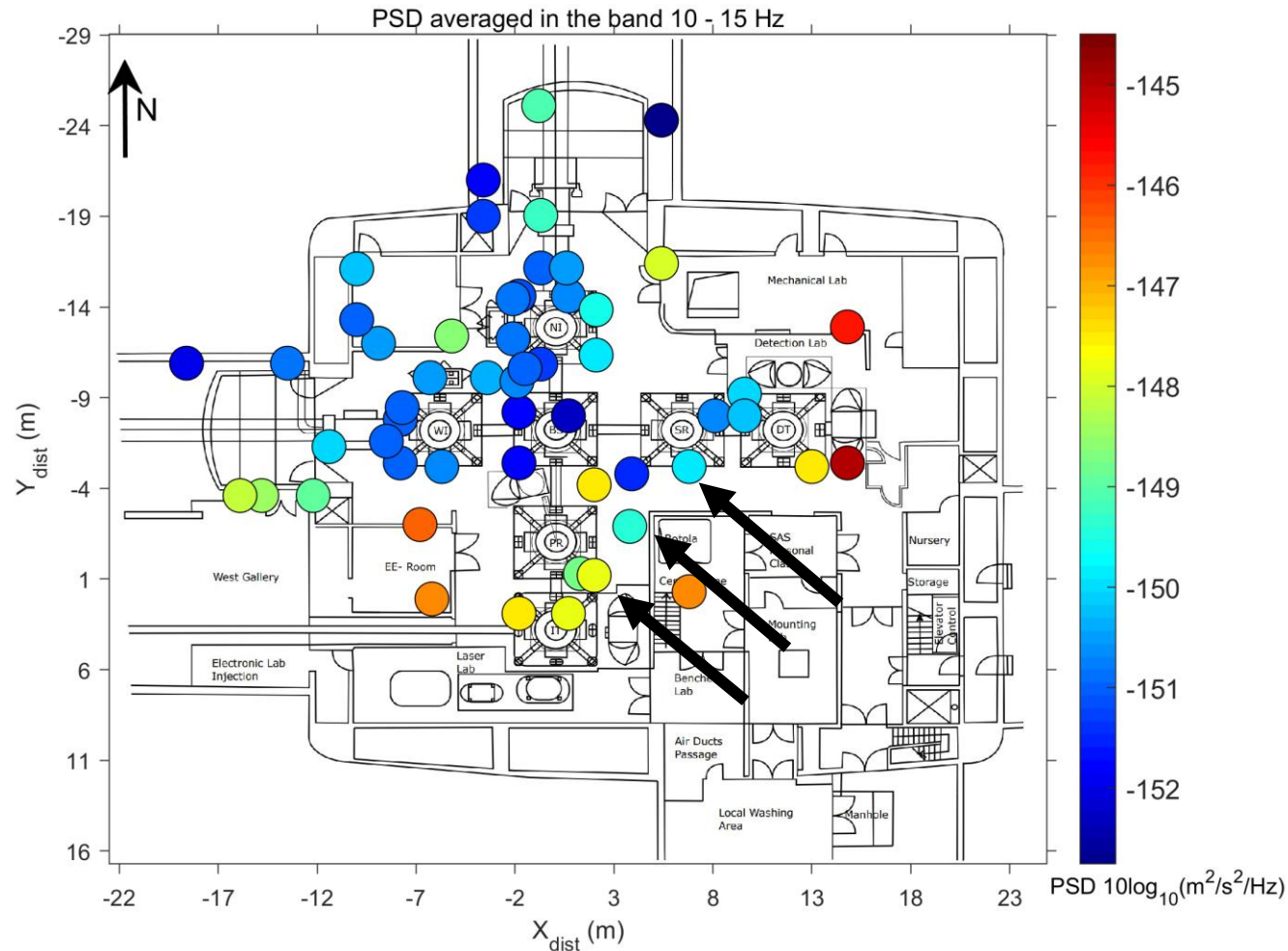# Noise PSD characteristics – Spatial variation for the 18.5 Hz noise peak
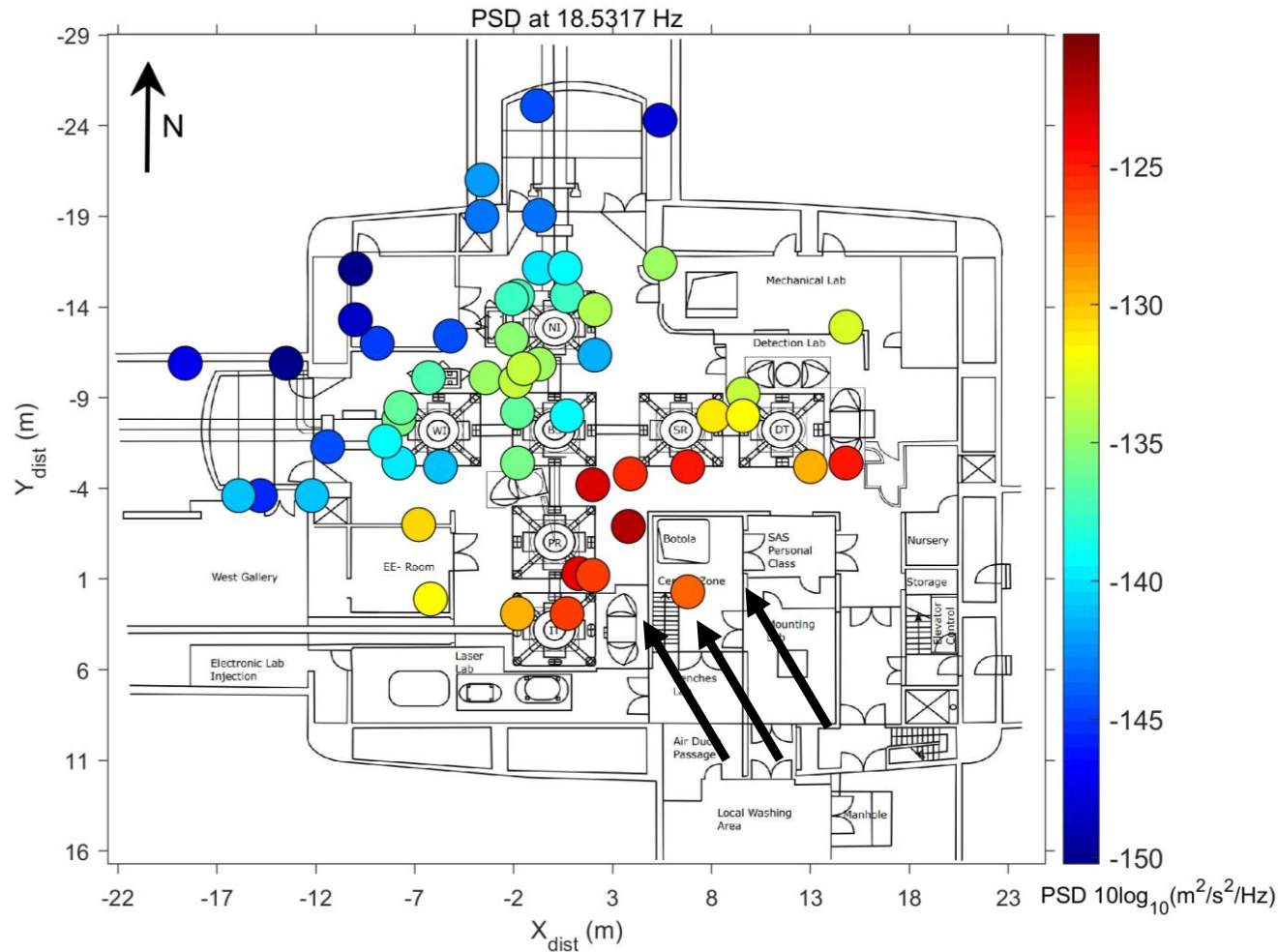
Spatial distribution of seismic noise PSDs for the peak at 18.5317 Hz

- Spatial variation of seismic noise PSDs can be used to infer location of noise sources within the building

- String PSD variation of about 30 dB observed

- Spatial variation of the noise PSDs for the 18.5317 Hz shows a dominant SSE-NNW

- Supply fan of the Air Handling Unit located in the CEB cleanroom has already been identified to be the source of this noise (https://tds.virgo-gw.eu/?content=3&r=20911)

Noise phase characteristics – normalized interstation cross-correlations

- Normalized cross-correlation between stations i and j for M windows can be expressed as

$$CC_{ij} = \text{real}\left(\frac{\sum_{k=1}^{M} X_i(f)X_j^*(f)}{\sqrt{\sum_{k=1}^{M} X_i(f)X_i^*(f) \sum_{k=1}^{M} X_j(f)X_j^*(f)}}\right), \text{ where } X(f) = \text{fft}(x(t))$$

Normalized frequency-domain cross-correlation of all 1485 station pairs in the CEB NNC array
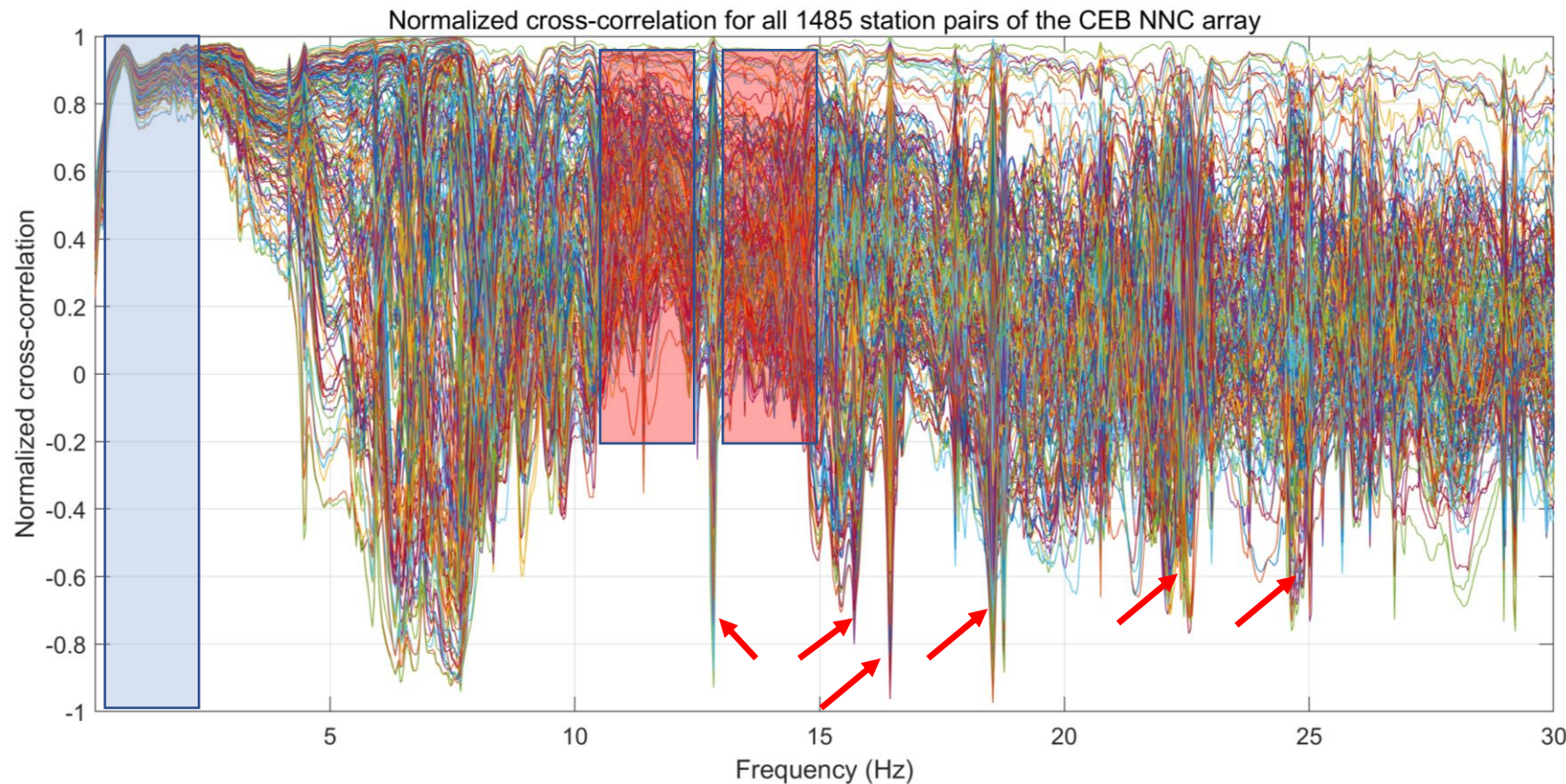
- Cross-correlations >=0.8 for the frequency band 0.4-3 Hz

- Dominated by anisotropic distribution of surface wave sources

- Mixture of horizontally and near-vertical propagating waves (body waves)

  - Cross-correlation functions with no zero-crossing

Noise phase characteristics – cross-correlations for anisotropic noise source distribution

- For any noise source distribution between azimuth ϕ_1 and ϕ_2 and vertical angle θ_1 and θ_2, the theoretical CCF can be expressed as

  - $CCF = \sum_{\theta=\theta_1}^{\theta=\theta_2} \sum_{\phi=\phi_1}^{\phi=\phi_2} F(\theta, \phi, f) \cos(\frac{2\pi f}{V}(sin\theta\ cos\phi\ \hat{\imath}\ + sin\theta\ sin\phi\ \hat{\jmath} + cos\theta\ \hat{k})(\vec{r_i} - \vec{r_j}))$ **s.t.** $\sum_{\theta=\theta_1}^{\theta=\theta_2} \sum_{\phi=\phi_1}^{\phi=\phi_2} F(\theta, \phi, f) = 1$
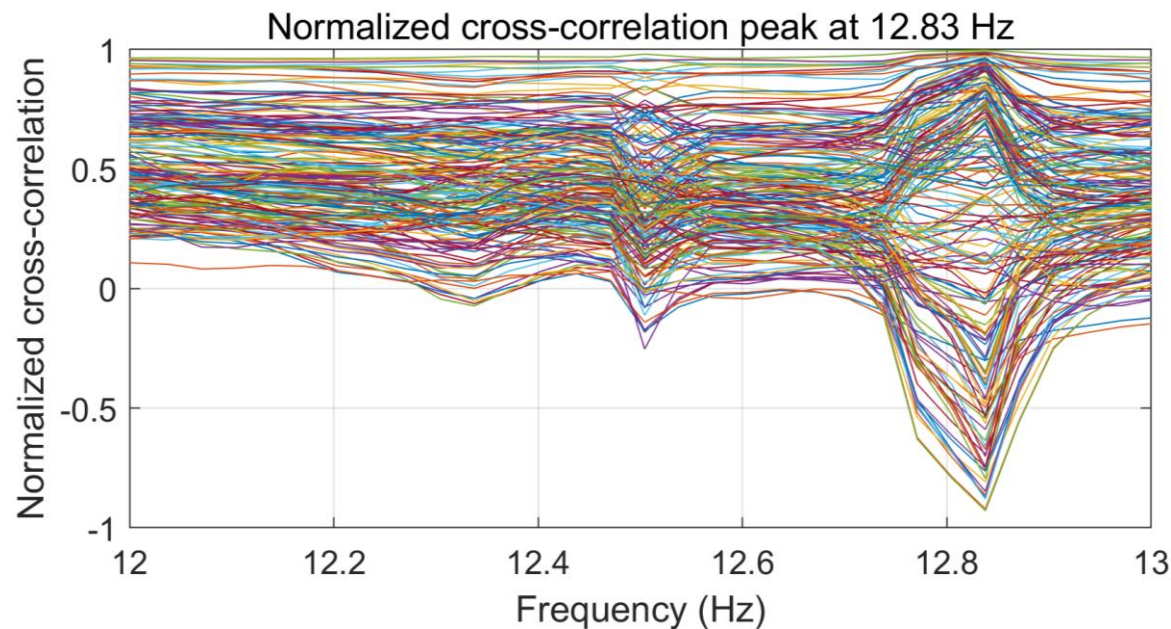
Beamform

Frequency domain cross-correlation corresponding to the peak at 12.8376 Hz, showing strong positive (≈ 1), and negative (≈ -1) correlations
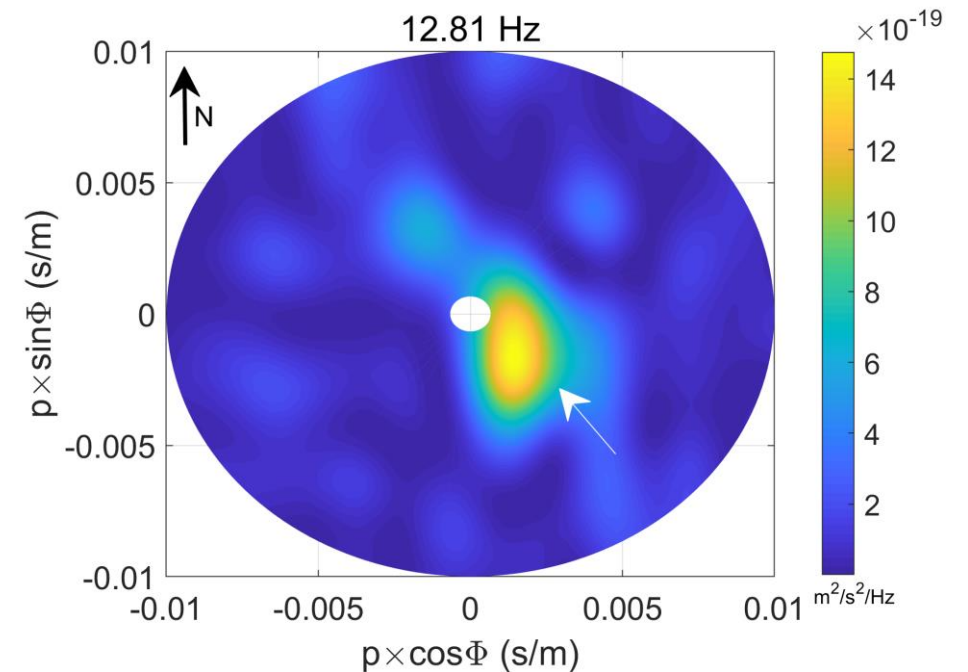
Beampower expressed in polar coordinates (p, ϕ) showing a dominant plane wave propagation between azimuths $290° - 340°$

Noise phase characteristics – spatial distribution of cross-correlation for 12.81 Hz peak
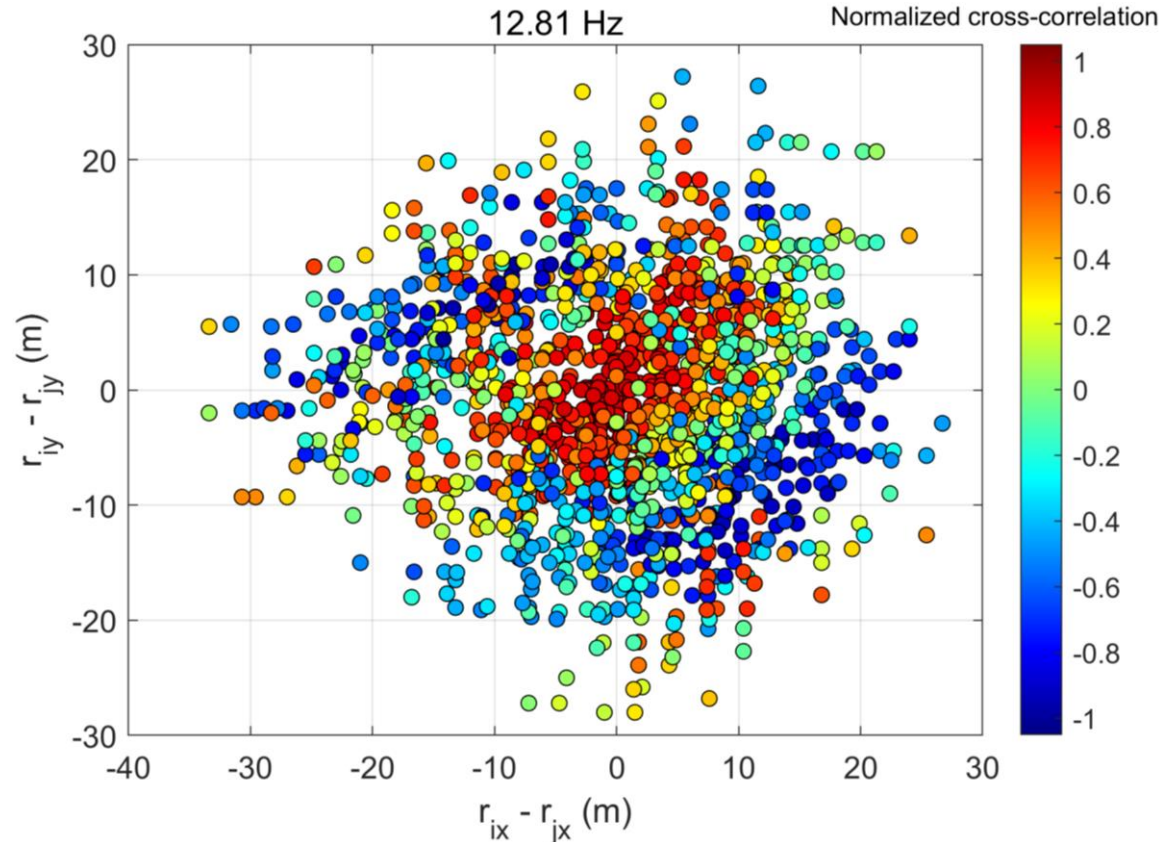
Spatial distribution of noise cross-correlations at 12.8 Hz show a horizontally propagating wave
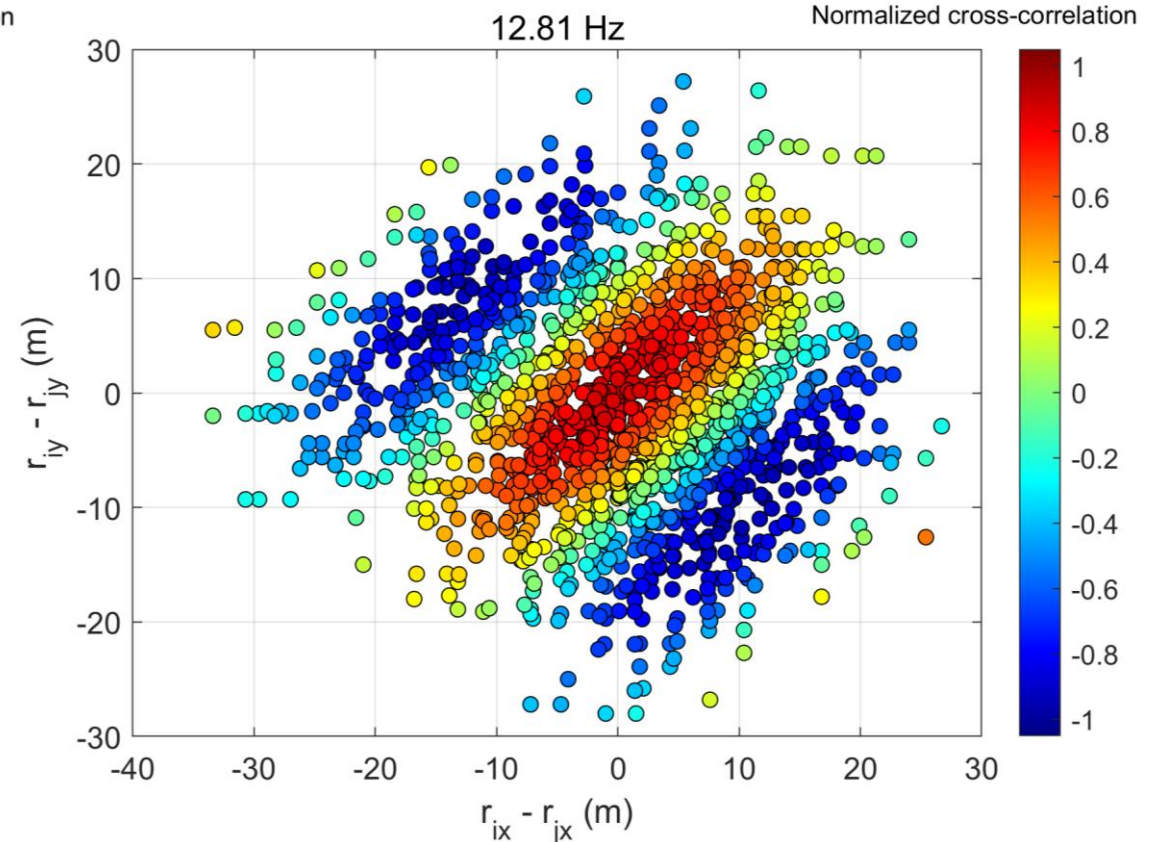
Spatial distribution of theoretical noise cross-correlations for a dominantly horizontally propagating wave at V = 370 m/s. $\phi_1 = 290^0$, $\phi_2 = 340^0$

Wiener filter – NN prediction

- Given P input channels (geophones) and a filter h of L coefficients, the predicted NN can be expressed as
  - $y_{NN} = \sum_{p=1}^{P} \sum_{m=0}^{L} x_{n-m}^{p} h_{m}^{p}$, where x_{k}^{p} is the kth input sample of the pth geophone

- Since y_{NN} is not available, assuming $y_{DARM} \approx y_{NN}$, the optimal filter h is a solution to the problem
  - $\min[(y_{DARM} - y_{NN})^2] \Rightarrow \min\left[\left(y_{DARM} - \sum_{p=1}^{P} \sum_{m=0}^{L-1} x_{n-m}^{p} h_m\right)^2\right]$

- Using the Wiener-Hopf formulation, the optimal filter h can be expressed as,
  - $h = R^{-1} Q$

where $R = \begin{pmatrix} \phi_{11} & \phi_{12} & \cdots & \phi_{1P} \\ \phi_{21} & \phi_{22} & & \phi_{2P} \\ \vdots & & \ddots & \vdots \\ \phi_{(P-1)1} & \phi_{(P-1)2} & \cdots & \phi_{(P-1)P} \\ \phi_{P1} & \phi_{P2} & & \phi_{PP} \end{pmatrix}$ $\Longrightarrow$ Full Rank

and $\phi_{ij} = \begin{pmatrix} C_{ij}(0) & C_{ij}(1) & \cdots & C_{ij}(L-1) \\ C_{ij}(-1) & C_{ij}(0) & & C_{ij}(L-2) \\ \vdots & & \ddots & \vdots \\ C_{ij}(-L+2) & C_{ij}(-L+1) & & C_{ij}(1) \\ C_{ij}(-L+1) & C_{ij}(-L) & \cdots & C_{ij}(0) \end{pmatrix}$, $C_{ij}(\tau) = x(t)x(t+\tau)$

$Q = \begin{pmatrix} \phi_{1y} \\ \phi_{2y} \\ \phi_{3y} \\ \cdot \\ \cdot \\ \cdot \\ \cdot \\ \cdot \\ \cdot \\ \phi_{Py} \end{pmatrix}$

Noise cancellation steps

- The first second output is not possible

```
                    ┌────────────────────┐         ┌────────────────────┐
                    │  Seismometer input │ ◄─────── │  Buffer 101 samples│
                    │     (500 Hz)       │ ◄──┐     │    (FIR order-1)   │
                    └────────────────────┘    │     └────────────────────┘
                              │                │
                              ▼                └──┐  ┌──────┐ ┌──────┐ ┌─────┐ ┌──────┐
┌────────────────────┐  ┌────────────────────┐   └─►│SEISM₁│ │SEISM₂│ │ ....│ │SEISMₙ│
│ Low Pass FIR filter│─►│ Decimate input     │      └──────┘ └──────┘ └─────┘ └──────┘
│ Order 20 × dec rate│  │    (100 Hz)        │
└────────────────────┘  └────────────────────┘
                              │
                              ▼
                        ┌────────────────────┐
                        │  Detrend input     │
                        └────────────────────┘
```

Seismometer input (500 Hz)

Buffer 101 samples (FIR order-1)

Low Pass FIR filter
Order $20 \times dec\ rate$

Decimate input (100 Hz)

SEISM$_1$ SEISM$_2$ .....   SEISM$_N$

Detrend input

Scaling factors during training

Scaling

5Hz Highpass (FIR)

Wiener or Adaptive coeff

LFilter using Wiener coeff, or CNN filter

Poly-resampling

Upsample To Target channel

Add all wiener/CNN filtered seismometer channels

Subtract from Target channel
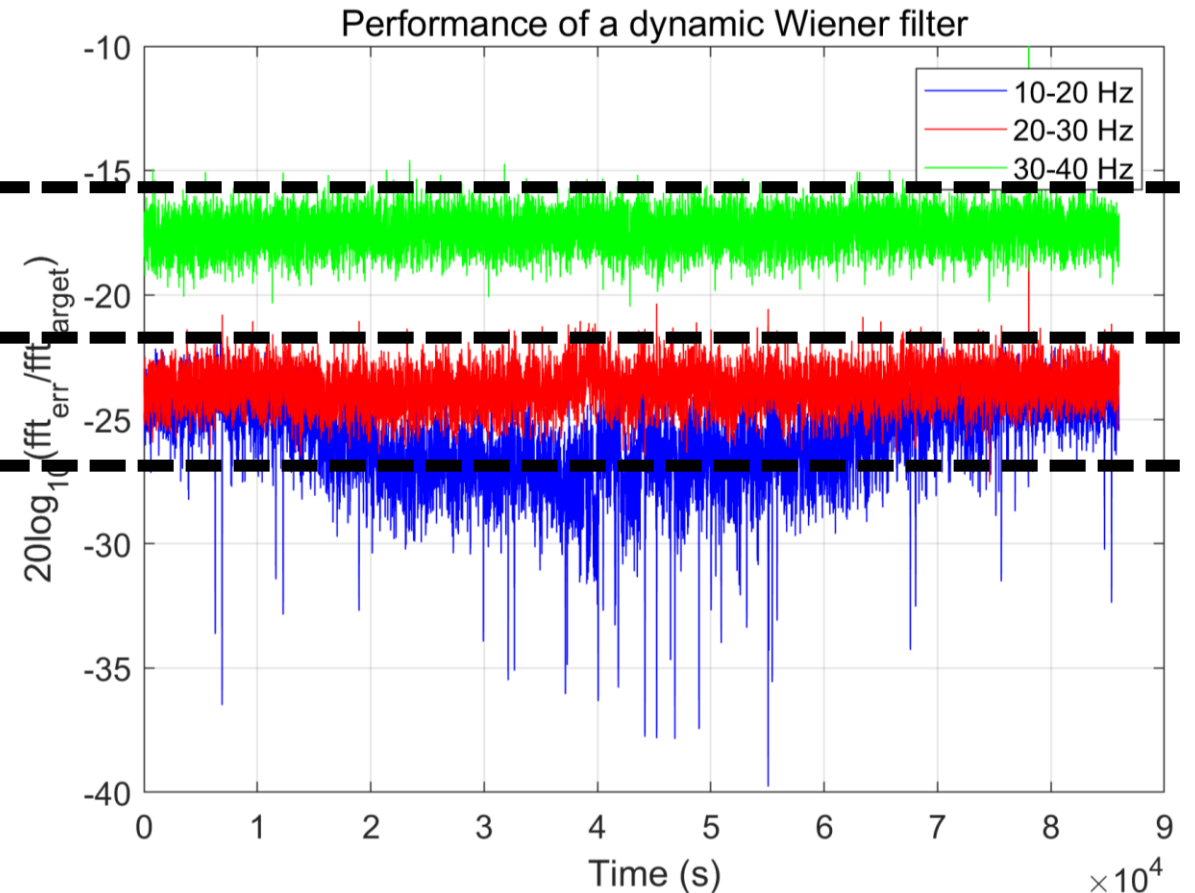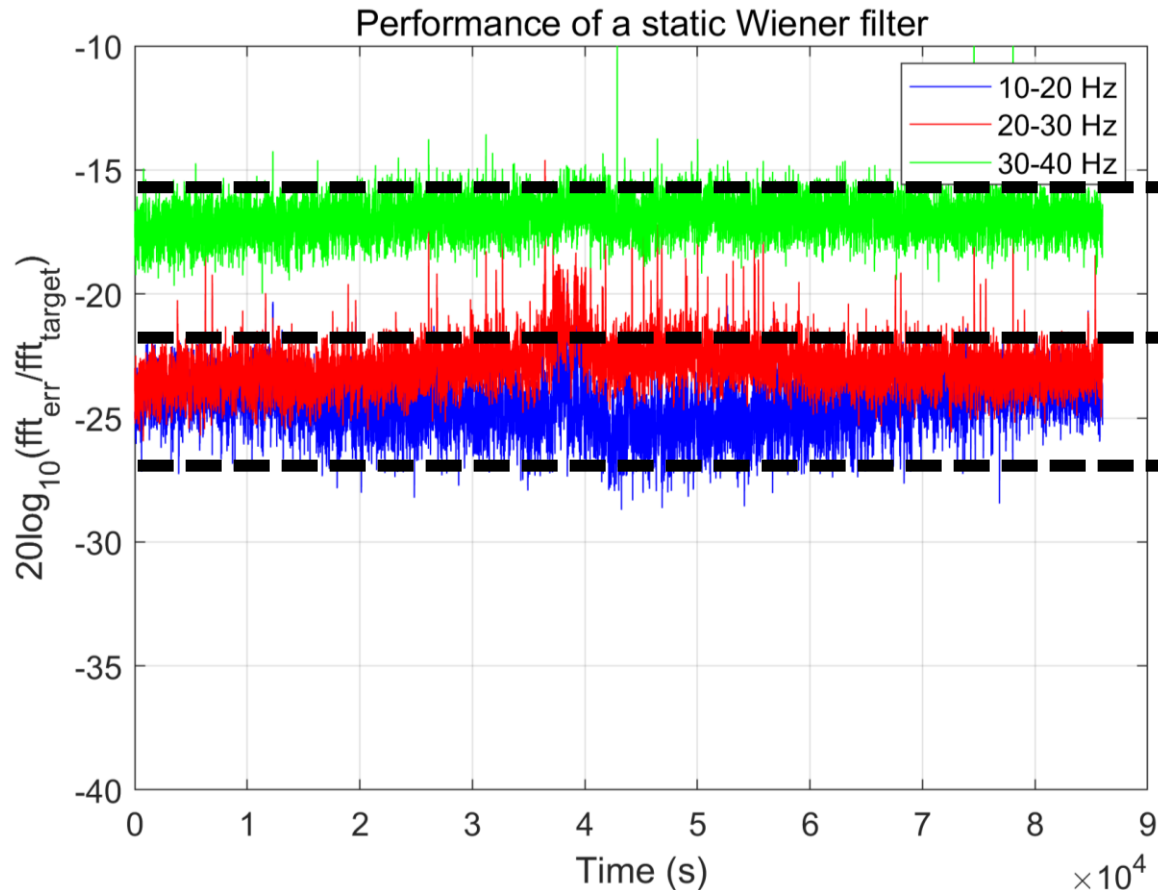
Wiener filter – Static vs Dynamic (CEB_SEIS_V as target)

- 10-20 Hz ➡ 25-27 dB
- 20-30 Hz ➡ 20-25 dB
- 30-40 Hz ➡ 16-18 dB

- About 10 dB better performance for transients
- About 2 dB better performance for transients
- Similar performance in 30-40 Hz band

Adaptive filters

- Two broad classes of algorithms exist for solving the Wiener problem:

- Least Mean Square (LMS/NLMS)

  - Stochastic gradient method ($O(LP)$)

  - $h(n) = h(n-1) + \mu(n)x(n-1)e(n)$
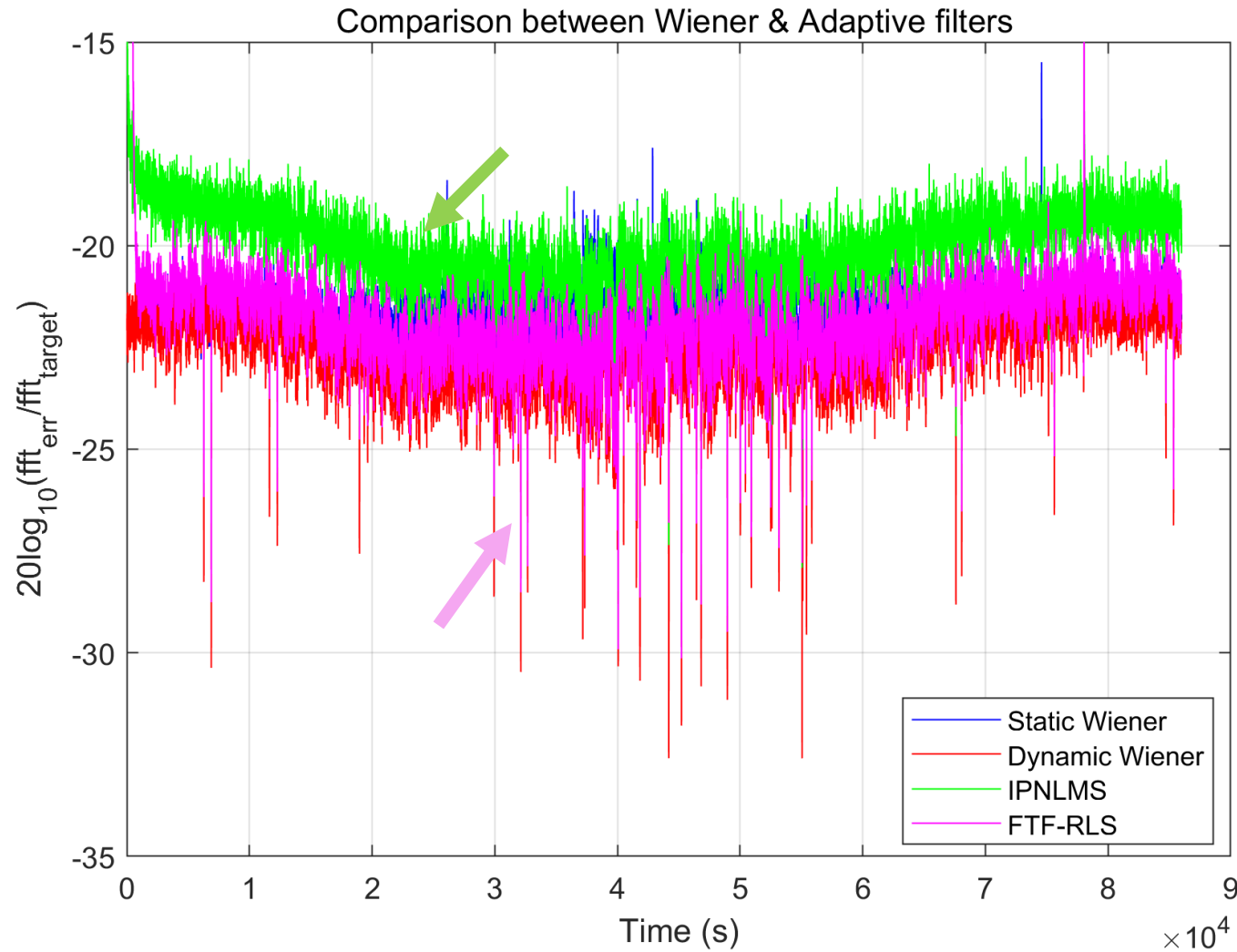   - $\mu(n) = \frac{\alpha}{x(n)x^T(n)+\delta}, 0 < \alpha < 2, \delta \approx 0$

- IPNLMS ([Improved proportionate NLMS](#))
- $\mu(k) = \frac{\alpha}{\sum_{m=0}^{L-1} x^2(k-m)g_{ip,m}(k-1)+\delta_{IPNLMS}}$

- $g_{ip,l}(k-1) = \frac{1-\beta}{2L} + (1+\beta)\frac{h_l(k-1)}{2\|\mathbf{h}(k-1)\|_1+\epsilon}$
- $\epsilon \approx 0, -1 \leq \beta < 1$

- Recursive least square (RLS)

  - $\min(\sum_{m=0}^{L-1} \lambda^{n-m}e^2(m))$

  - $h(n) = h(n-1) + R_{xx}^{-1}(n)x(n)e(n)$ (Gauss-Newton like)

  - $R_{xx}^{-1}(n) = \lambda^{-1}R_{xx}^{-1}(n-1) - \frac{\lambda^{-2}R_{xx}^{-1}(n-1)x(n)x^T(n)R_{xx}^{-1}(n-1)}{1+\lambda^{-1}x(n)R_{xx}(n-1)x^T(n)}$

  - Complexity $\approx O(L^2P^2)$ per sample (not feasible)

  - Stabilized Fast Transversal algorithms ([Slock and Kailath, 1991](#))
    - $O(LP)$
    - Solves the exact quadratic problem
    - Good tracking even in noisy environment
    - Computationally expensive

Wiener vs Adaptive filters (CEB_SEIS_V as target)

Comparison between Wiener & Adaptive filters

Legend:
- Static Wiener (blue)
- Dynamic Wiener (red)
- IPNLMS (green)
- FTF-RLS (magenta)

- IPNLMS performs about 4 dB worse than Wiener/Dynamic-Wiener during quiet times
- During short-burst transients IPNLMS does better than static Wiener filter but worse than Dynamic Wiener or FTF-RLS

- Performance of FTF RLS comparable to the dynamic Wiener filter

Wiener vs Adaptive filters at the onset (CEB_SEIS_V as target)

Comparison between Wiener & Adaptive filters
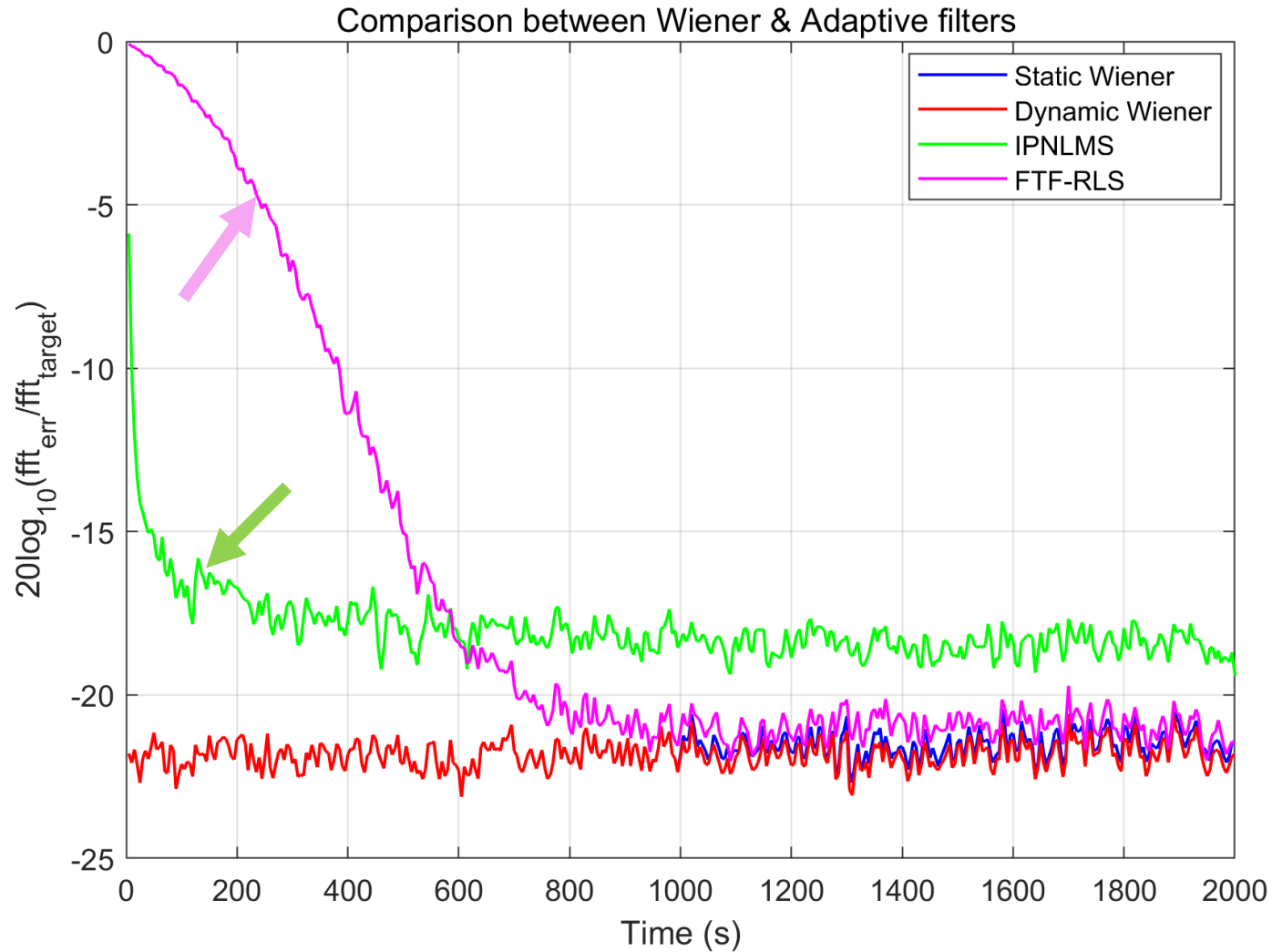
- IPNLMS converges quickly for $\alpha = 0.5$, and $\beta = -0.75$

- FTF RLS takes a bit longer ($\approx 800s$) to reach steady state, but performs comparable to the dynamic Wiener filter
- Slow convergence is due to $\lambda = 1 - \frac{1}{LP}$ (≈ 1)
- However, if λ is made smaller, the numerical stability of the algorihm is compromised

Wiener vs Adaptive filters during transients (CEB_SEIS_V as target)

Comparison between Wiener & Adaptive filters for transients
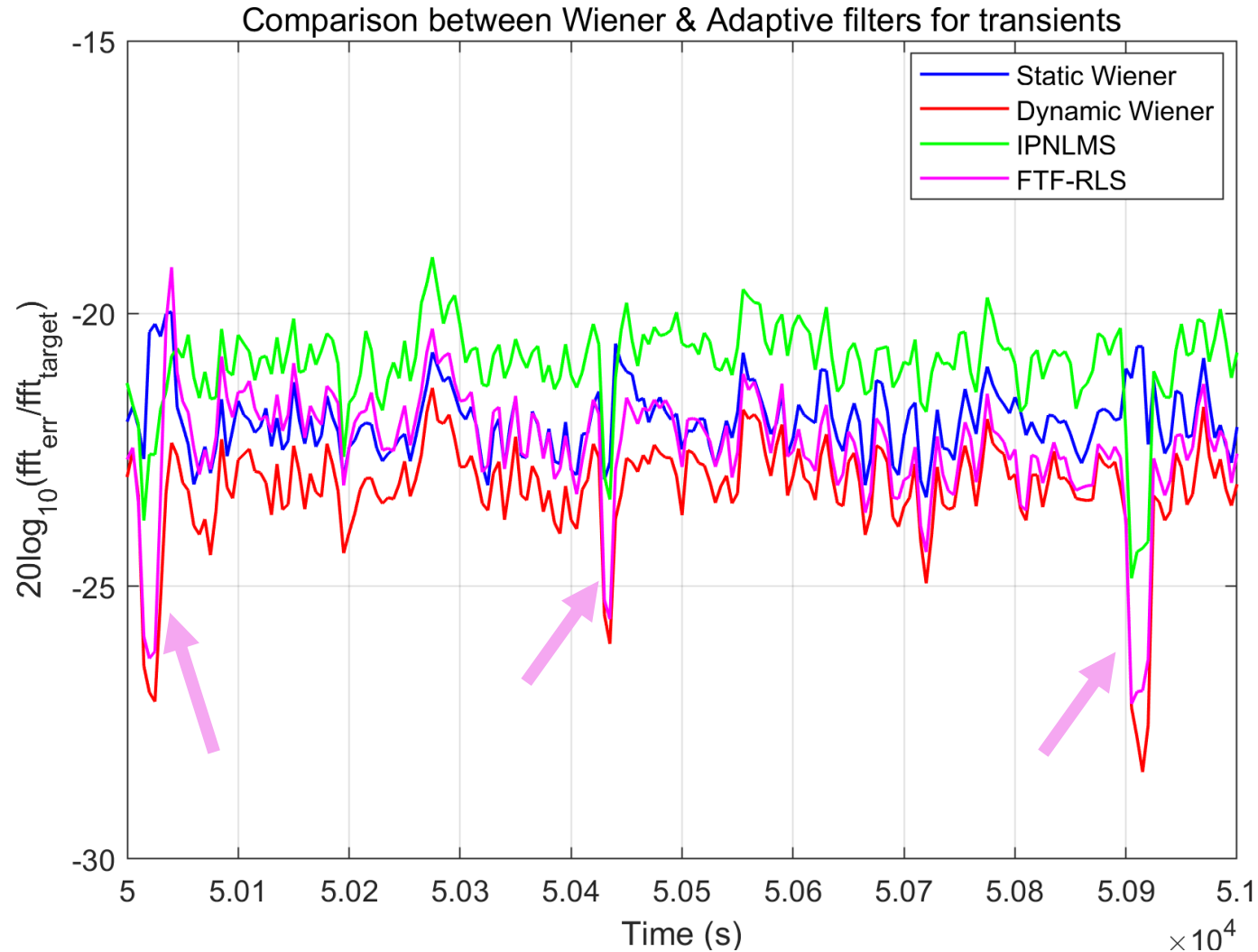
- FTF RLS performs within a dB of the dynamic Wiener filter

- During quiet-times its performance is between the static and the dynamic Wiener filters

- Performance can be improved by modifying the rescue procedure
  - Soft-constrained initialization is in play
  - Decorrelate inputs to stabilize the condition number of the forward and backward predictor matrices

Wiener vs Adaptive filters (CEB_SEIS_N as target)

Comparison between Wiener and Adaptive filters with CEB SEIS N as target
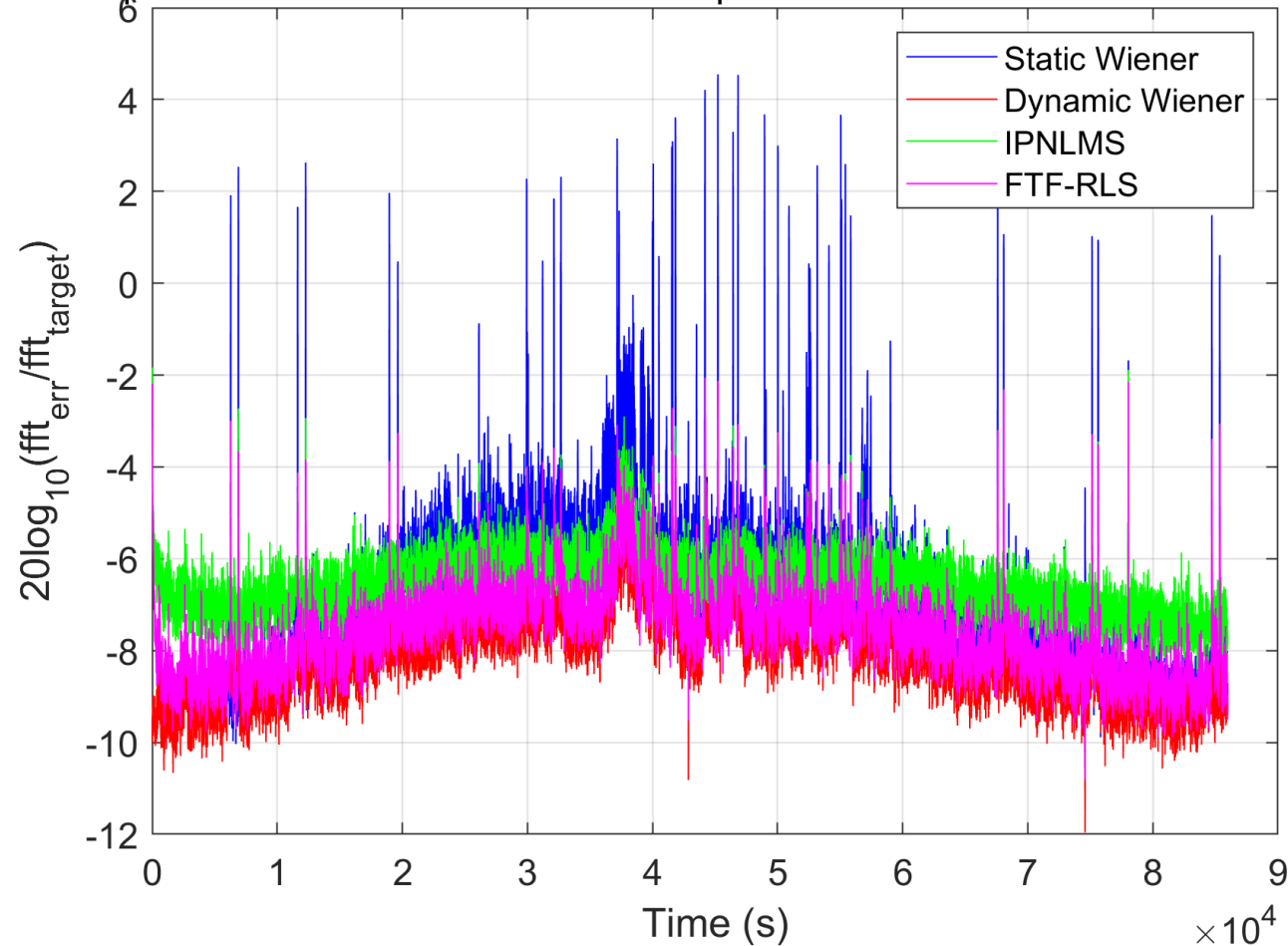
- Maximum gain of about 10 dB during quiet times (was 25 dB for V-target)
- Performance worse by about 2-3 dB during noisy-times
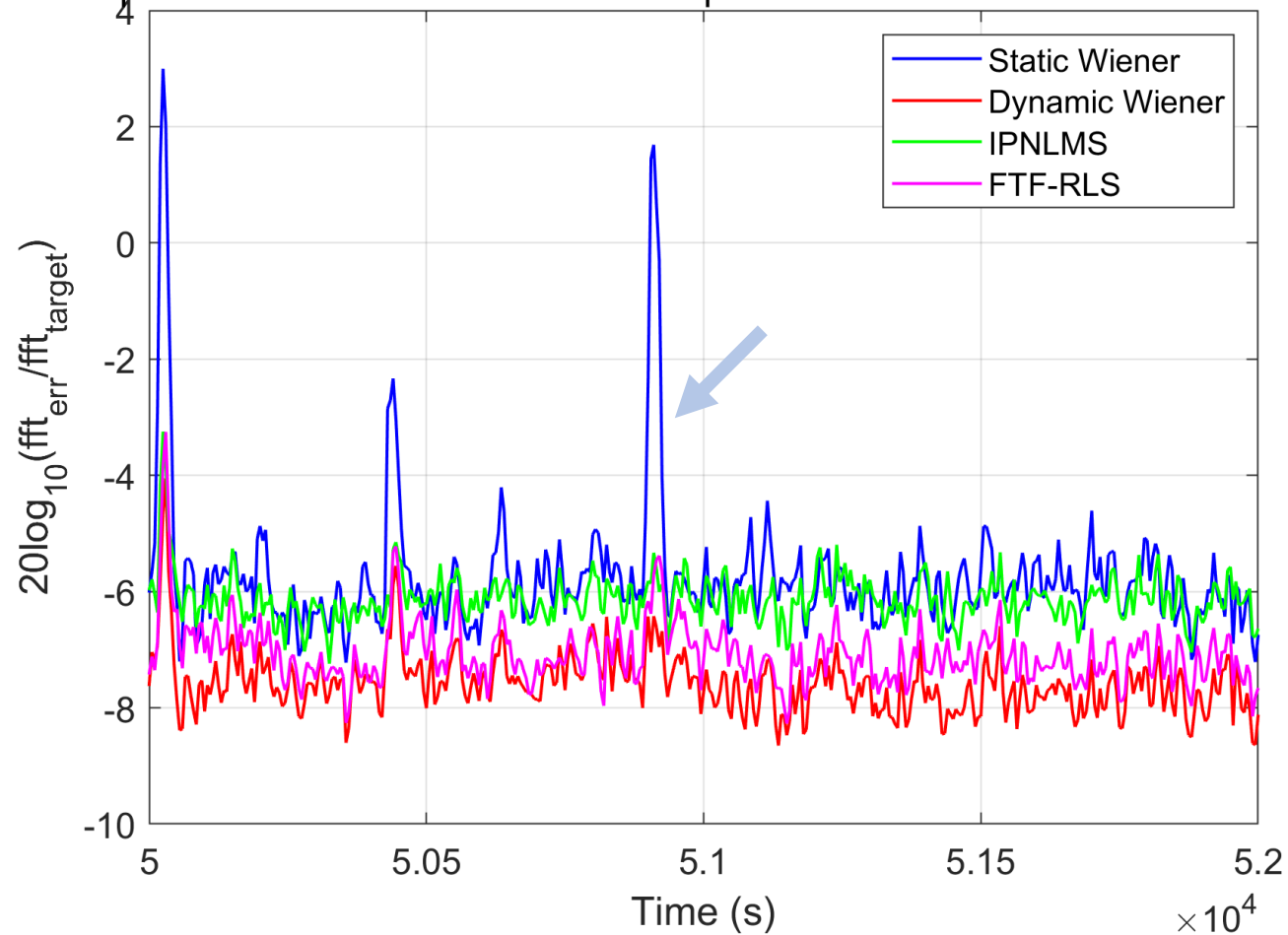
- Static Wiener filter performance worse for transients
  - Unfavorable wave-types

- IPNLMS performance comparable to or better than FTF-RLS for transients
- Performance worse by 3-4 dBs during quiet-times

- Performance of FTF RLS comparable to dynamic Wiener filter performance

Wiener vs Adaptive filters during transients (CEB_SEIS_N as target)

Comparison between Wiener and Adaptive filters with CEB SEIS N as target

- During noisy times, performance of all algorithms are comparable except for the static Wiener filter, which adds noise to the data-stream

- FTF RLS performance is close to dynamic Wiener filter and outperforms IPNLMS marginally ($1 - 2$ dB)

- Overall cancellation of the horizontal channel using vertical channels as input is a challenging problem and is a scenario similar to NN-cancellation

Conclusions

- 55 vertical component 4.5 Hz geophones in the CEB, 28 in the NEB and 30 in the WEB were installed
- Data digitization at 500 sps performed within the sensors and data readout was integrated with the Virgo DAQ system (time synchronized)

- Sensor locations - optimization studies based on seismic wavefield characteristics and simulated NN were performed

- An online NNC implementation has been done based on the static Wiener filter case (https://git.ligo.org/virgo/virgoapp/NNCfilter/-/tree/NNCTest01)

- Adaptive filter options were explored: LMS (different classes) and RLS (FTF, FLA)
- FTF-RLS were found to be robust, and were tested offline
- Performance could be enhanced by designing better rescue algorithms

- A challenging problem of subtracting the horizontal seismic noise channel by using the vertical channel was considered
  - Gain of about 10 dB during quiet times and about 7-8 dB during noisy times could be achieved
  - Performance worse by about 15 dB compared to the scenario when the vertical channel was used as target

Questions?